Effect of solid obstacle and thermal conditions on convective flow and entropy generation of nanofluid filled in a cylindrical chamber

H.A. Kumara Swamy
Department of Mathematics, Nonlinear Dynamics and Mathematical Application Center, Kyungpook National University, Daegu, Republic of Korea

Sankar Mani
Department of Information Technology, University of Technology and Applied Sciences – Ibri, Ibri, Oman and Department of Mathematics, Presidency University, Bangalore, India

N. Keerthi Reddy
Department of Mechanical Engineering, Ulsan National Institute of Science and Technology, Ulsan, Republic of Korea, and

Younghae Do
Department of Mathematics, Nonlinear Dynamics and Mathematical Application Center, Kyungpook National University, Daegu, Republic of Korea

Abstract
Purpose – One of the major challenges in the design of thermal equipment is to minimize the entropy production and enhance the thermal dissipation rate for improving energy efficiency of the devices. In several industrial applications, the structure of thermal device is cylindrical shape. In this regard, this paper aims to explore the impact of isothermal cylindrical solid block on nanofluid (Ag – H$_2$O) convective flow and entropy generation in a cylindrical annular chamber subjected to different thermal conditions. Furthermore, the present study also addresses the structural impact of cylindrical solid block placed at the center of annular domain.

Design/methodology/approach – The alternating direction implicit and successive over relaxation techniques are used in the current investigation to solve the coupled partial differential equations. Furthermore, estimation of average Nusselt number and total entropy generation involves integration and is achieved by Simpson and Trapezoidal's rules, respectively. Mesh independence checks have been carried out to ensure the accuracy of numerical results.

Findings – Computations have been performed to analyze the simultaneous multiple influences, such as different thermal conditions, size and aspect ratio of the hot obstacle, Rayleigh number and nanoparticle

shape on buoyancy-driven nanoliquid movement, heat dissipation, irreversibility distribution, cup-mixing temperature and performance evaluation criteria in an annular chamber. The computational results reveal that the nanoparticle shape and obstacle size produce conducive situation for increasing system's thermal efficiency. Furthermore, utilization of nonspherical shaped nanoparticles enhances the heat transfer rate with minimum entropy generation in the enclosure. Also, greater performance evaluation criteria has been noticed for larger obstacle for both uniform and nonuniform heating.

Research limitations/implications – The current numerical investigation can be extended to further explore the thermal performance with different positions of solid obstacle, inclination angles, by applying Lorentz force, internal heat generation and so on numerically or experimentally.

Originality/value – A pioneering numerical investigation on the structural influence of hot solid block on the convective nanofluid flow, energy transport and entropy production in an annular space has been analyzed. The results in the present study are novel, related to various modern industrial applications. These results could be used as a firsthand information for the design engineers to obtain highly efficient thermal systems.

Keywords Annular chamber, Buoyant convection, Cup-mixing temperature, Entropy generation, Hot obstacle, Nanoparticle shape

Paper type Research paper

Nomenclature

Be = Bejan number;
C_p = Specific heat [J/(kg K)];
d = Width of the obstacle [m];
D = Width of the annulus [m];
FFE = Entropy due to fluid friction;
g = Acceleration due to gravity [m/s^2];
h = Height of the obstacle [m];
H = Height of the annulus [m];
HTE = Entropy due to heat;
k = Thermal conductivity [W/(m K)];
$\overline{Nu}$ = Average Nusselt number;
p = Dimensional pressure [Pa];
P = Dimensionless pressure;
Pr = Prandtl number;
r_i and r_o = Dimensional radius of inner and outer cylinders [m];
(r, z) = Dimensional radial, axial coordinates [m];
(R, Z) = Dimensionless radial, axial coordinates;
Ra = Rayleigh number;
S_{GEN} = Local entropy generation;
S_{tot} = Total entropy generation;
t^* = Dimensional time [s];
t = Dimensionless time;
T = Dimensionless temperature;
T_{cup} = Cup-mixing temperature;
(u, w) = Dimensional radial, axial velocity components [m/s]; and
(U, W) = Dimensionless radial, axial velocity components.

Greek letters
α = Thermal diffusivity [m2/s];
β = Thermal expansion coefficient [K^{-1}];
Γ = Aspect ratio of obstacle;

θ = Dimensional temperature [K];
λ = Radius ratio;
μ = Dynamic viscosity [kg/(ms)];
ν = Kinematic viscosity [m^2/s];
ρ = Density [kg/m^3];
ϕ = Nanoparticle volume fraction;
ψ = Stream function; and
ζ = Vorticity.

Subscripts
c = Cold;
f = Base fluid;
h = Hot; and
nf = Nanofluid.

1. Introduction

The convective motion and associated thermal dissipation along with entropy generation (EG) in a differently heated finite-sized geometry are the crucial parameters in the design of many important thermal devices. Therefore, several investigations have been focused on buoyant heat transfer analysis inside a finite-shaped geometry due to its relevance in numerous industrial applications, which include storage tanks, room ventilation, double pane windows, heat exchangers, cooling of containment buildings, electronic cooling and solar collectors. In addition, an enclosed annular geometry formed by two concentric cylinders, among various finite-shaped geometries, aptly mimics important applications ranging from nuclear reactors to the complicated industrial equipment (Lopez and Marques, 2014). One of the pioneering works on experimental study of convective heat dissipation of various liquids in an annulus region by considering three aspect ratios has been made by Prasad and Kulacki (1985). The partial heating influence on fluid motion as well as heat transport in an annular chamber has been examined by Sankar and Do (2010) by taking various constraints into consideration and predicted that thermal dissipation could be improved with partial heating, and placing the thermal source at an appropriate location could also enhance the heat transport.

In recent years, utilization of liquids dispersed with nanosized solid particles having higher thermal conductivity, known as nanoliquids, is preferred to increase the heat transfer rate (HTR) in several industrial applications (Choi and Eastman, 1995; Godson *et al.*, 2010). Abouali and Falahatpisheh (2009) considered a vertical annulus and made a pioneering investigation of Al$_2$O$_3$-water nanofluid flow and heat transport rates. They presented heat dissipation correlations for square as well as annular cavities. The impact of different base fluids on fluid motion as well as HTR in an annulus containing nanofluid has been analyzed by Mebarek-Oudina (2019) and reported that HTR of TiO$_2$-nanofluid greatly depends on the choice of base fluid. The investigation of two-phase dusty nanofluid movement in an annular space has been carried out by Saha *et al.* (2020) and found that the density ratio and the dusty parameter play key role in optimization of HTR. By adopting finite volume method, the convective heat transport in an annulus containing Cu-water nanofluid containing an inner rotating circular cylinder has been numerically studied by Mirzaie and Lakzian (2021) and concluded that enhancement of angular velocity leads to an increase in HTR. Berrahil *et al.* (2021) studied buoyant convection of nanoliquid in an annulus considering the axial as well as radial magnetic field influences and proposed correlations for global heat dissipation in terms of radius ratio, nanoparticle concentration, Rayleigh and

Hartmann numbers. Recently, the effect of different nanoparticles on fluidity and thermal dissipation rate under various constraints has been investigated and proposed the suitable combination of parametric values to improve HTR in the annular domain (Reddy *et al.*, 2021; Lakshmi *et al.*, 2021).

A finite-sized enclosure accommodating a solid obstacle of different shapes has been a topic of several investigations due to the relevance in numerous practical applications, such as building designing, electronic component cooling, thermal insulation and solar collectors. One of the pioneering studies on fluid motion and thermal transport in a cavity containing solid heat conducting body has been performed by House *et al.* (1990). They reported that enclosure containing small size obstacle results in maximum dissipation of thermal energy. Kim *et al.* (2008) adopted the immersed boundary technique to predict the influence of inner cylinder location on HTR and fluid flow strength in a square geometry. Ragui *et al.* (2013) addressed the size effects of hot obstacle on convective HTR in a cavity and proposed a correlation for average Nusselt number as a function of block size and Rayleigh number. Natural convection and thermal transport in a nanofluid-filled cavity containing different obstacles, such as square adiabatic block by Mahmoodi and Sebdani (2012) and hot cylindrical block by Esfe *et al.* (2014), have been investigated to identify the shape impacts of obstacle. It has been predicted that the aspect ratio of adiabatic square block and radius of inner circular block could significantly control the fluid motion and heat transfer process. By using the lattice Boltzmann method, Rahmati and Tahery (2018) analyzed the conductive solid block influence mounted at the central region of the enclosure by maintaining high temperature along the bottom surface and obstacle boundaries and found an optimum obstacle location to enhance the HTR. In recent times, analyzing the liquid flow and resulting energy transport rates in the cavity containing different shaped obstacle has received substantial attention which mainly discusses various outcomes pertaining to obstacle shape and size (Roy, 2019).

The aforementioned literature with/without obstacle focuses on the flow and thermal transport analysis by neglecting EG. Recently, the studies based on second-law (EG) have gained prime importance for a better understanding of system's thermal efficiency. EG has become one of the prime factors for estimating the efficiency of thermal devices because it quantifies the energy loss caused by irreversibility phenomenon (Bejan, 1982, 1996). Baytas (2000) made an attempt to investigate entropy due to fluid friction (FFE) and heat (HTE) in a porous inclined enclosure and observed that irrespective of Darcy–Rayleigh number, minimal FFE is noticed for 270° inclination of the cavity. In a similar geometry, Ilis *et al.* (2008) made a detailed analysis to address the thermal performance by assessing energy dissipation and EG. The production of entropy in any system could also be strongly altered from additional factors, such as magnetic field and multiple buoyancy forces. Recently, the impacts of discrete heating, source–sink location and annular tilt angle on nanofluid flow strength and HTR along with irreversibility analysis have been numerically examined by Sankar *et al.* (2023). It has been proposed that the smaller source–sink pairs with suitable choice of geometry inclination could enhance the HTR with minimal production of entropy. Shuja *et al.* (2000) made a pioneering attempt to numerically analyze the effect of solid block and its position on fluid flow (air/water), HTR and EG in a cavity. The obtained results shows that the enclosure filled with air generates higher entropy as compared to water. Sheikhzadeh *et al.* (2012) made computational analysis to address the impact of hot square block mounted at the central region of nanofluid-filled cavity and reported that an increase in the block size has better thermal efficiency (maximum HTR with minimum EG) at lower Rayleigh number. The influence of cylindrical isothermal body located at the central region of tilted enclosure has been analyzed on fluid flow and EG and found that decrease in

Prandtl number reduces total EG in the cavity (Mun *et al.*, 2016). Alsabery *et al.* (2018) studied the effect of solid adiabatic block on nanofluid movement, EG and HTR and reported that the optimization of system efficiency could be controlled by thermal conductivity ratio and block size.

Numerous scientific works have been performed to analyze the change in fluid flow pattern, HTR and EG under the influence of different constraints like effect of magnetic field, porous media, double diffusion, nonuniform heating, structure of the geometry, shape of obstacle and many others. Malik and Nayak (2017) numerically investigated the nonuniform thermal profile impact on magnetoconvective nanofluid flow and EG in a porous cavity and reported that the fractional increment of nanoparticles increases HTR very effectively. The hybrid nanoliquid motion in a square porous enclosure subjected to linear heating profile could be significantly controlled by applying Lorentz force at four different locations (Manna *et al.*, 2021). The Lorentz force tilt angle as well as solid block on thermal transport and fluid motion filled in a cavity under different thermal conditions has been numerically investigated (Pal *et al.*, 2022). Selimefendigil and Oztop (2015) examined the impact of obstacle shape, Lorentz force, internal heat generation on nanoliquid flow along with HTR and EG in a cavity and reported that selection of the parametric values play significant role to enhance the system efficiency. Tayebi and Chamkha (2020) reported that irrespective of Hartmann number, an enhancement in the conductivity ratio results in an enhancement in HTR and decrease in total EG of hybrid nanofluid contained in an enclosure containing wavy obstacle. Vijaybabu (2020) performed computational study to address the hot porous object impact on natural convective phenomena and irreversibilities in a cavity and found that the minimum EG depends on the permeability of cylinder. Kardgar (2021) examined the impact of Lorentz force on conduction–convection flow, thermal dissipation and EG of nanofluid filled in an inclined cavity. The collective effects of Lorentz force, chemical reaction and heat generation on the energy transport along with EG in a doubly stratified porous geometry have been studied by Kumar *et al.* (2022a, 2022b). Recently, the influence of magnetic field and porous medium on convective HTR and EG of *MWCNT* – H_2O nanoliquid has been studied by Kumar *et al.* (2022, 2022b) for different thermal conditions and concluded that heat transfer phenomenon is lower for linear thermal profile than constant heating case. As discussed above, the geometrical shape of the cavity plays a remarkable role in investigation of buoyancy-driven fluid flow, heat transport rate and EG. In some industries, the geometrical structure of the thermal device may be irregular, namely, C/U/L-shaped, parallelogram, triangular, quadrantal, wavy enclosure and various other odd shapes. By considering different constraints, numerical experiments have been performed to predict a suitable situation to maximize HTR and minimize EG in the abovementioned geometries (Sheremet *et al.*, 2017; Dogonchi and Hashim, 2019; Dogonchi *et al.*, 2021; Tayebi *et al.*, 2022).

1.1 Motivation

The thorough literature review regarding convective fluid flow and associated thermal transport rate along with EG subjected to different conditions has been made in aforementioned section. For better understanding, the earlier research works related to heat and fluid flow in various geometries containing obstacle have been displayed in Table 1. Through this, it has been found that *the existing works are mainly focused on square and other nonannular enclosures*. Also, the influence of hot solid block on the convective nanofluid flow, energy transport and EG in an annular space has not yet been attempted. The annular geometry, one of the most-sought geometries, aptly describes the physical structure of many important applications, such as electronic device cooling, nuclear reactors, heat exchangers, solar technology and dry-type transformers. The knowledge of flow, thermal distribution and EG rates of square cavity could not be used in these applications

Authors	Geometry	Fluid	Obstacle shape	Thermal conditions	Entropy generation
House et al. (1990)	Square	Air	Square (conductive)	Uniform	Not studied
Kim et al. (2008)	Square	Air	Circular (hot)	Uniform	Not studied
Mahmoodi and Sebdani (2012)	Square	$Cu - H_2O$	Square (adiabatic)	Uniform	Not studied
Esfe et al. (2014)	Square	$H_2O/Cu - H_2O/Al_2O_3 - H_2O$	Cylindrical (hot)	Uniform	Not studied
Rahmati and Tahery (2018)	Square	$TiO_2 - H_2O$	Square (hot)	Uniform	Not studied
Roy (2019)	Square	$Al_2O_3 - H_2O$	Wavy (hot)	Uniform	Not studied
Shuja et al. (2000)	Square	Air/H_2O	Square (hot)	Uniform	Studied
Sheikhzadeh et al. (2012)	Square	$Cu - H_2O$	Square (adiabatic)	Uniform	Studied
Mun et al. (2016)	Inclined cavity	$Pr = 0.01 - 100$	Cylindrical (hot)	Uniform	Studied
Alsabery et al. (2018)	Square	$Al_2O_3 - H_2O$	Square	Discrete	Studied
Pal et al. (2022)	Square	H_2O	Pair of cylindrical (hot)	Uniform	Not studied
Selimefendigil and Oztop (2015)	Square	$Cu - H_2O$	Circular, square and diamond (adiabatic)	Sinusoidal	Studied
Tayebi and Chamkha (2020)	Square	$Cu - Al_2O_3 - H_2O$	Corrugated (conductive)	Uniform	Studied
Vijaybabu (2020)	Square	$Cu - H_2O$	Permeable circular body	Uniform	Studied
Dogonchi and Hashim (2019)	Wavy	$Fe_3O_4 - H_2O$	Diamond	Uniform	Not studied
Dogonchi et al. (2021)	Wavy	$Fe_3O_4 - H_2O$	Pair of square (hot and cold)	Uniform	Studied
Tayebi et al. (2022)	Inclined I-shape	$Al_2O_3 - H_2O$	Pair of cylinders (hot)	Uniform	Studied

Source: Table by authors

Table 1.
Details of few
published works in
the presence of
obstacle

due to curvature effect of annular geometry. For better understanding, the comparison between average Nusselt number for square and annular enclosure has been made for various obstacle sizes, nanoparticle shape and thermal conditions are displayed in Table 2. Due to the greater difference in HTR between square and annular enclosures, and also due to many industrial applications of annular enclosure, it is essential to investigate the impact of isothermal obstacle on nanoliquid flow, heat dissipation and EG in an annular enclosure. The numerical approach and validation have been provided in Section 3. The simulations have been carried out for a wide range of parameters such as Rayleigh number (Ra: 10^3–10^5), obstacle size (δ: 0.2–0.7) and aspect ratio (Γ: 0.5–2) by considering different nanoparticle shapes and thermal conditions, and the outcomes are discussed in Section 4. Finally, the key findings of this numerical investigation are summarized in Section 5.

2. Problem formulation

The physical domain considered in this analysis is a 2D annular geometry structured from two vertical and coaxial cylinders with r_i and r_o as the radii of inner and outer cylinders, respectively. The space between cylinders is filled with silver–water nanofluid (Table 3 depicts H$_2$O and nanoparticle properties). The inner and outer cylinders are kept at low temperature, the top boundary is retained as insulated and three different higher thermal conditions (uniform/linear/sinusoidal heating represented as Case-I/Case-II/Case-III) are imposed along the bottom wall. Also, a uniformly heated cylindrical solid block has been placed at the center of annular domain as shown in Figure 1. The widths of annulus and solid block are, respectively, taken as D and d, and the heights of annulus and solid block are, respectively, denoted as H and h. In this study, the single-phase model, which was first adopted by Choi and Eastman (1995), is used because the nanoparticle concentration is sufficiently low, resulting in minimal or negligible pressure drop difference when compared to a single-phase fluid. It is also assumed that the dispersed nanoparticles in the base fluid have a uniform morphology, and both phases (solid and liquid) are in a thermal equilibrium condition (Hamzah and Sahin, 2023). Therefore, the nanofluid is considered as a homogeneous fluid with improved thermal properties, whose values are determined using the models presented in Table 4 (Yan *et al.*, 2020; Dogonchi *et al.*, 2021; Kumar *et al.*, 2023). Also, it has been assumed that the fluid is Newtonian and incompressible with unsteady, laminar and axisymmetric flow. The Boussinesq approximation is assumed. Viscous dissipation is neglected but EG is considered. These type of assumptions have been chosen from Rosca *et al.* (2023).

2.1 Governing equations

As per the conservative laws and postulates, the dimensional modeled equations are as follows:

$$\nabla.\ \overrightarrow{q} = 0, \tag{1}$$

$$\rho_{nf}\left[\frac{\partial \overrightarrow{q}}{\partial t^*} + \left(\overrightarrow{q}.\nabla\right)\overrightarrow{q}\right] = -\nabla p + \mu_{nf}\nabla^2\overrightarrow{q} + (\rho\beta)_{nf}\ \overrightarrow{g}\,(\theta - \theta_c), \tag{2}$$

$$\frac{\partial \theta}{\partial t^*} + \left(\overrightarrow{q}.\nabla\right)\theta = \alpha_{nf}\nabla^2\theta, \tag{3}$$

The dimensionless variables used in the present investigation are as follows:

Ra	d	h	Nanoparticle shape	$\overline{Nu}$ for uniform heating		$\overline{Nu}$ for linear heating		$\overline{Nu}$ for sinusoidal heating	
				Square	Annulus	Square	Annulus	Square	Annulus
10^3	0.3	0.3	Spherical	6.5850331	8.6840452	2.4697965	3.5717699	1.0253931	1.1978497
	0.7	0.7		5.4124021	7.3932065	0.1665528	0.6840464	−0.8060156	−0.8510240
	0.4	0.2		6.3933114	8.4490096	2.0429081	3.0509654	1.0366892	1.198037
	0.2	0.4		6.4145126	8.4699332	1.8297109	2.9326275	0.9167009	1.1781592
	0.2	0.2	Blade	5.4226164	7.3144455	3.9354729	6.8763990	1.7235268	3.4629886
			Brick	4.8811030	6.0213484	3.3589613	5.6603438	1.4772871	2.8447513
			Cylinder	4.1988443	5.2196701	2.4855416	4.7548948	0.5143560	1.8449354
			Platelet	4.5177621	5.4174346	2.5764136	4.9393388	0.5493479	1.9306888
10^5	0.3	0.3	Spherical	10.8924231	13.0776185	4.3255926	6.0068852	5.1441646	5.3626164
	0.7	0.7		5.7227195	7.8802541	0.5779625	1.0902441	−0.2383840	−0.3069542
	0.4	0.2		9.7130774	12.8864425	3.7230911	5.9637697	3.9676952	5.2081197
	0.2	0.4		10.1843720	13.0783448	3.7900560	5.9619294	4.2962653	5.3501909
	0.2	0.2	Blade	7.2448242	9.5343485	5.9788348	8.6290111	4.5972134	5.9911304
			Brick	5.5370105	7.9756457	5.2099922	7.1929093	3.9933995	5.0518617
			Cylinder	4.0114265	6.2455630	4.9763937	5.7453685	2.3086142	3.2028743
			Platelet	4.7904321	6.3325629	4.9624523	5.8654660	2.1241894	3.1830767

Source: Table by authors

Table 2.
Comparison between
heat transfer rate of
square and annular
enclosure for
different thermal
conditions

$$(R, Z) = \frac{(r, z)}{D}, \quad U = \frac{uD}{\alpha_f}, \quad W = \frac{wD}{\alpha_f}, \quad t = \frac{t^* \alpha_f}{D^2}, \quad T = \frac{(\theta - \theta_c)}{(\theta_h - \theta_c)}, \quad P = \frac{pD^2}{\rho_{nf} \alpha_f^2}.$$

By using the aforementioned dimensionless variables, nondimensional energy and vorticity–stream function equations are expressed as below:

$$\frac{\partial T}{\partial t} + U \frac{\partial T}{\partial R} + W \frac{\partial T}{\partial Z} = \frac{\alpha_{nf}}{\alpha_f} \nabla^2 T \tag{4}$$

$$\left[\frac{\partial \zeta}{\partial t} + U \frac{\partial \zeta}{\partial R} + W \frac{\partial \zeta}{\partial Z} - \frac{U\zeta}{R} \right] = \frac{\mu_{nf}}{\rho_{nf} \alpha_f} \left[\nabla^2 \zeta - \frac{\zeta}{R^2} \right] - \frac{(\rho\beta)_{nf}}{\rho_{nf} \beta_f} \, Ra \, Pr \, \frac{\partial T}{\partial R} \tag{5}$$

$$\zeta = \frac{1}{R} \left[\frac{\partial^2 \psi}{\partial R^2} - \frac{1}{R} \frac{\partial \psi}{\partial R} + \frac{\partial^2 \psi}{\partial Z^2} \right] \tag{6}$$

where:

$$U = \frac{1}{R} \frac{\partial \psi}{\partial Z}, \; W = -\frac{1}{R} \frac{\partial \psi}{\partial R}, \; \nabla^2 = \frac{\partial^2}{\partial R^2} + \frac{1}{R} \frac{\partial}{\partial R} + \frac{\partial^2}{\partial Z^2}, \; Ra = \frac{g\beta_f \Delta\theta D^3}{\nu_f \alpha_f} \; \text{and} \; Pr = \frac{\nu_f}{\alpha_f}.$$

The dimensionless BCs imposed are as follows:

Material	ρ (kg/m^3)	C_p (J/kg K)	k (W/mK)	$\beta \times 10^5$ (K^{-1})
H$_2$O	997.1	4179	0.613	21
Ag	10500	235	429	1.89

Source: Saha *et al.* (2020) and Belhaj and Ben-Beya (2022)

Table 3.
Water and
nanoparticle
properties
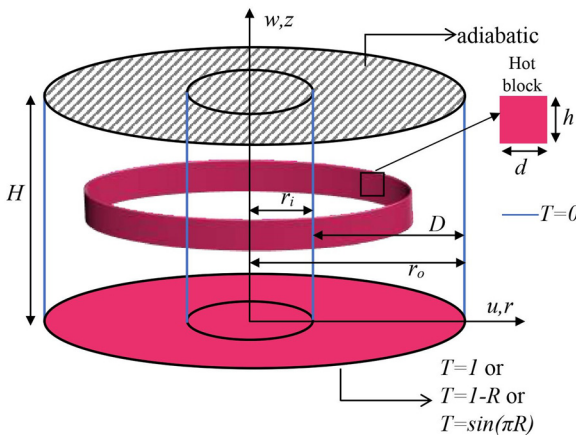
Source: Figure by authors

Figure 1.
Physical domain and
its axisymmetric
representation

Nanofluid properties	Applied model			
Thermal expansion coefficient	$(\rho\beta)_{nf} = \phi(\rho\beta)_p + (1-\phi)(\rho\beta)_f$			
Density	$\rho_{nf} = (1-\phi)\rho_f + \phi\rho_p$			
Heat capacitance	$(\rho C_p)_{nf} = (1-\phi)(\rho C_p)_f + \phi(\rho C_p)_p$			
Thermal diffusivity	$\alpha_{nf} = \dfrac{k_{nf}}{(\rho C_p)_{nf}}$			
Thermal conductivity	$\dfrac{k_{nf}}{k_f} = \dfrac{k_p + (n-1)k_f - (n-1)\phi(k_f - k_p)}{k_p + (n-1)k_f + \phi(k_f - k_p)}$, for nonspherical nanoparticles			
	$\dfrac{k_{nf}}{k_f} = \dfrac{k_p + 2k_f - 2\phi(k_f - k_p)}{k_p + 2k_f + \phi(k_f - k_p)}$, for spherical nanoparticles			
Dynamic viscosity	$\mu_{nf} = \mu_f\left(1 + A_1\phi + A_2\phi^2\right)$, for nonspherical nanoparticles			
	$\mu_{nf} = \dfrac{\mu_f}{(1-\phi)^{2.5}}$, for nanoparticles with spherical shape			
Shape of the nanoparticle	χ	$n = 3/\chi$	A_1	A_2
Blade	0.36	8.6	14.6	123.3
Cylinder	0.62	4.9	13.5	904.4
Platelet	0.52	5.7	37.1	612.6
Brick	0.81	3.7	1.9	471.4

Sources: Yan *et al.* (2020); Dogonchi *et al.* (2021); Kumar *et al.* (2023)

Table 4.
Equations for estimating nanofluid properties

For $t > 0$:

$$\psi = \frac{\partial\psi}{\partial R} = 0, \ T = 0;$$

at vertical surfaces:

$$\psi = \frac{\partial\psi}{\partial Z} = 0, T = 1 \,(\text{or}) \, 1 - R \,(\text{or}) \sin(\pi R);$$

at bottom surface:

$$\psi = \frac{\partial\psi}{\partial Z} = 0, \ \frac{\partial T}{\partial Z} = 0;$$

at top surface:

$$\psi = \frac{\partial\psi}{\partial\eta} = 0, T = 1;$$

at solid block. Here, η denotes normal to a boundary of the hot block.

2.2 Entropy generation equation
In any system, as per the second law, transfer of heat occurring due to temperature gradients causes irreversibility and produce entropy. The irreversibilities are exhibited from

heat transport as well as friction due to fluid flow. According to local thermodynamic equilibrium with linear transport theory, the dimensional form of EG can be given by:

$$S_{gen} = \frac{k_{nf}}{\theta_0^2} \left[\left(\frac{\partial \theta}{\partial r} \right)^2 + \left(\frac{\partial \theta}{\partial z} \right)^2 \right] + \frac{\mu_{nf}}{\theta_0} \left[2 \left\{ \left(\frac{\partial u}{\partial r} \right)^2 + \left(\frac{u}{r} \right)^2 + \left(\frac{\partial w}{\partial z} \right)^2 \right\} + \left(\frac{\partial u}{\partial z} + \frac{\partial w}{\partial r} \right)^2 \right]$$

(7)

By using the dimensionless variables, the nondimensional form of HTE ($S_{l.T}$) and FFE ($S_{l.\Psi}$) is given by:

$$S_{l.T} = \frac{k_{nf}}{k_f} \left[\left(\frac{\partial T}{\partial R} \right)^2 + \left(\frac{\partial T}{\partial Z} \right)^2 \right]$$

$$S_{l.\Psi} = \Phi \frac{\mu_{nf}}{\mu_f} \left[2 \left\{ \left(\frac{\partial U}{\partial R} \right)^2 + \left(\frac{U}{R} \right)^2 + \left(\frac{\partial W}{\partial Z} \right)^2 \right\} + \left(\frac{\partial U}{\partial Z} + \frac{\partial W}{\partial R} \right)^2 \right],$$

(8)

where the corresponding irreversibility distribution ratio (Φ) is defined as:

$$\Phi = \frac{\mu_f}{k_f} \theta_0 \left(\frac{\alpha_f}{D\Delta\theta} \right)^2.$$

The local EG in an annular region is equal to the sum of HTE and FFE which is defined as:

$$S_{GEN} = S_{l.T} + S_{l.\Psi}$$

(9)

The overall heat dissipation rate along the bottom surface, represented by the average Nusselt number, is defined as (Alsabery *et al.*, 2018):

$$\overline{Nu} = -\left(\frac{k_{nf}}{k_f} \right) \int \frac{\partial T}{\partial Z} \, dR$$

The thermal mixing in the annulus is estimated by cup-mixing temperature and is defined as follows (Kumar *et al.*, 2022, 2022b):

$$T_{cup} = \frac{\iint \hat{W}(R,Z) T(R,Z) R \, dR \, dZ}{\iint \hat{W}(R,Z) R \, dR \, dZ}$$

here,

$$\hat{W}(R,Z) = \sqrt{U^2 + W^2}.$$

The total EG is evaluated by integrating equation (9) within the geometry and is estimated from the following equation:

$$S_{tot} = \frac{1}{V} \int_V S_{GEN} \ dV = \frac{1}{V} \int_V (S_{l.T} + S_{l.\Psi}) \ dV \tag{10}$$

Equation (10) can be written as $S_{tot} = S_T + S_\Psi$. The contribution of HTE and FFE has been estimated by Bejan number (Be_l) which is given by:

$$Be_l = \frac{S_{l,T}}{S_{GEN}} \tag{11}$$

The overall Bejan number is given by integration of equation (11) within the enclosure:

$$Be = \frac{1}{V} \int_V Be_l \ dV. \tag{12}$$

In addition, to estimate the dominance of HTR over EG or vice versa in buoyant convection problems, the quantity known as performance evaluation criteria (PEC) has been evaluated by $PEC = \overline{Nu}/S_{tot}$ (Malik and Nayak, 2017).

3. Computational procedure, grid test and validation

The governing PDEs (4–6) together with initial and boundary constraints are solved by adopting an implicit finite difference technique. Specifically, vorticity as well as temperature equations have been solved by implementing the alternative direction implicit technique, and equation (6) has been solved using the SLOR iterative method. A detailed description of these two methods is elaborately discussed in recent papers (Reddy et al., 2021; Reddy and Sankar, 2023). Thomas algorithm procedure has been used to invert the tri-diagonal linear system of equations. Further by using higher order central difference approximation, equations (8) and (9) are solved to estimate the local EG due to individual components. Finally, the overall HTR and total EG are calculated by using Simpson and Trapezoidal's rules, respectively. Table 5 displays $\overline{Nu}$ and S_{tot} for different grid sizes, and it reveals that the mesh size of 201×201 is suitable for further simulations. The comparison is very important in any computational study for verifying the accuracy of simulation code. In this regards, the comparison of streamlines and isotherms between the current result and the study of Rahmati and Tahery (2018) which deals with flow and heat distribution of nanoliquid in a square enclosure containing solid block is displayed in Figure 2(a). In addition to this, validation of HTE, FFE and S_{GEN} with Ilis et al. (2008) is reported in Figure 2(b). Furthermore, the average Nusselt number obtained from the current model is compared with the values from previously conducted experimental studies (Hamad, 1989) for a

| Mesh size	$\overline{Nu}$	Relative difference	S_{tot}	Relative difference
51×51	11.1270533	–	73.8762198	–
101×101	12.0741732	0.07844	74.4945199	0.008299
201×201	13.0776185	0.07672	75.0047046	0.006802
251×251	13.2082124	0.00988	75.2261110	0.002943

Source: Table by authors

Table 5.
Grid independency study

cylindrical annulus. The results of this comparison are presented in Table 6. From the aforementioned two comparisons, the outcomes from current simulation code hold good with the predictions of existing benchmark solutions and provide confidence to carry out further simulations.

4. Results and discussion

4.1 Streamlines, isotherms and entropy generation (S_{GEN})

The influence of Ra on flow, thermal and EG distributions are illustrated in Figure 3 for water and nanoliquid with a fixed hot block size. The analysis has been carried out for two Ra values (meager $Ra = 10^3$ and stronger 10^5), representing the conduction and convection dominant modes, respectively. Due to the presence of centrally mounted heated block, the fluid and thermal distributions are significantly altered. Hence, the flow structure appears to be in bicellular pattern for both Rayleigh numbers with clockwise fluid flow on the right and counterclockwise fluid flow on the left of hot block. This is due to thermal gradients generated between the cold vertical walls and centrally mounted hot block. At lower Ra, due to conduction dominant, the fluidity is minimal and also the addition of nanoparticles has not revealed any major change in the flow strength. However, as Ra is enhanced, the buoyant force enhances and in turn convection mode takes place due to which the fluidity of both water and nanoliquid has been increased. As regard to isotherms, at lower Ra, the isopleths of temperature are parallel to gravity, representing that the heat transport takes

(a) **(b)**
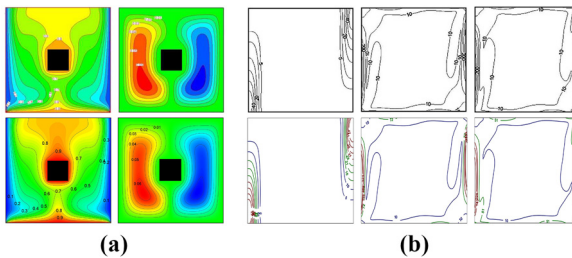
Notes: (a) Shows comparison of thermal and flow lines between current work (bottom) and results of Rahmati and Tahery (2018) (top); (b) presents comparison of HTE (left), FFE (middle) and SGEN (right) of current study (bottom) with Ilis *et al*. (2008) (top)
Source: Rahmati and Tahery (2018) and Ilis *et al*. (2008)

Figure 2.
Validation of current results with existing benchmark problems

Ra	Average Nusselt number ($\overline{Nu}$)		Relative difference (%)
	Hamad (1989)	Present study	
5×10^4	6.584	6.551	0.50
1×10^5	6.863	6.812	0.74
1.5×10^5	7.033	6.992	0.58
2×10^5	7.155	7.149	0.83

Source: Hamad (1989)

Table 6.
Comparison of $\overline{Nu}$ obtained from the present study with experimental findings in a cylindrical annulus filled with air ($Pr = 0.71$)
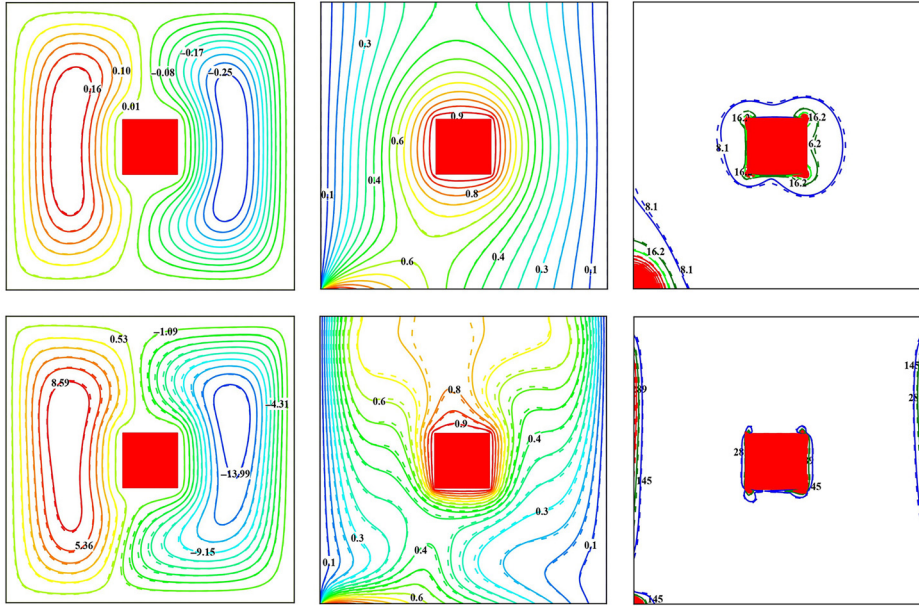
Figure 3.
Streamlines (left),
isotherms (middle)
and S_{GEN} (right) for
$Ra = 10^3$ (row-I),
$Ra = 10^5$ (row-II) at
$d = h = 0.2$, $\phi = 0$
(dotted line), $\phi = 0.04$
(solid line) with linear
heating

Source: Figure by authors

place by conduction mode. However, on enhancing the Ra value, a significant change in contour pattern of isotherms has been observed, indicating a strong buoyant flow, and hence higher heat dissipation takes place by convection mode. Along with flow and isotherm field, the EG has also been estimated and presented. The predictions revealed that at lower Ra value, the EG takes place only near higher temperature regions (i.e. around hot block and bottom left corner) and is due to the slow movement of fluid in the enclosure. However, on increasing the Rayleigh number, the flow strength enhances and results in higher production of entropy, which also spreads near cold wall region.

Figure 4 illustrates the effect of hot block size on fluid motion, thermal and EG contour patterns with $Ra = 10^5$, $\Gamma = 1$ and $\phi = 0.04$. The size of hot block is varied from 0.3 to 0.7, and, as discussed earlier, the fluid flow takes place in bicellular flow pattern for each block size. It has been observed that as the block size is enhanced, the fluidity declines due to transition in heat transfer mode. For smaller block size, the area occupied by the nanofluid is larger and hence generates higher convective heat transfer. However, as the block size is enhanced, most of the annular region is filled with hot block, and this creates a narrow region between the cold wall and hot obstacle, which suppress the convective flow. Due to this, the fluidity decreases with an enhancement in the block size. This can also be justified through isotherms which reveal a nearly parallel isotherms in the narrow gap between the block and vertical surfaces of the annulus. As regards to irreversibility distribution, an enhancement in the size of hot block declines EG, as the nanoliquid flow strength decreases with the size of hot block. Because EG depends on the velocity gradient of the nanoliquid [refer equation (9)], as flow strength decreases, FFE drops down considerably and produces lower irreversibility in the enclosure. In particular, it has been noticed that enhancement of hot block size from 0.3 to 0.7 causes 24.41% decline in EG.
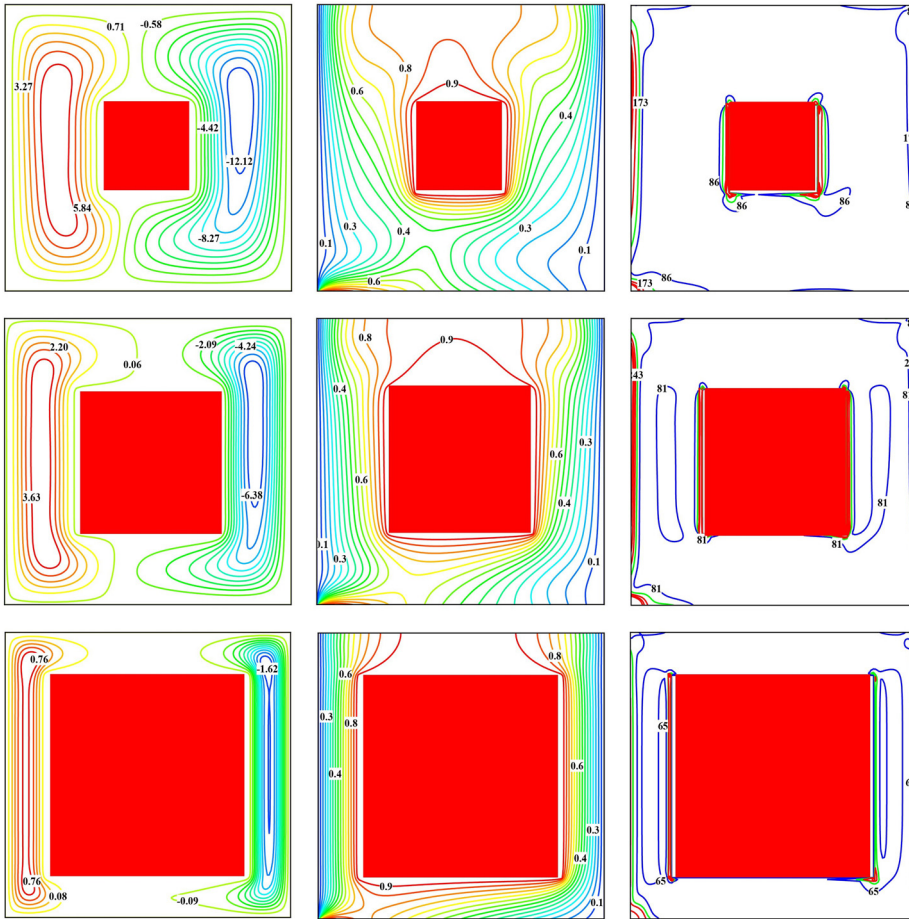
Source: Figure by authors

The influence of Γ on fluid motion, thermal as well as distribution of entropy with linear bottom wall heating has been represented in Figure 5 by keeping $Ra = 10^5$ and $\phi = 0.04$. Due to hot block mounted at the center of the annulus, a two-eddy nanoliquid flow exists with one rotating in clockwise and other in counterclockwise direction. For shallow hot block ($d = 0.4$, $h = 0.2$), the eddy size closer to inner wall is smaller compared to the eddy near outer wall. However, on varying the aspect ratio of hot block, the size of inner eddy enhances, whereas the outer wall eddy remains nearly of the same size. It is also interesting to note that the strength of inner eddy enhances with block aspect ratio, while the strength of outer eddy increases from shallow to square block, but declines with tall block. From the magnitude of streamlines, it has been found that the fluidity is greater in the annulus with square block compared to shallow and tall blocks. For similar conditions, the isotherm contours are clustered adjacent to the vertical isothermal walls as well as the hot block, indicating the existence of thermal boundary layer. Also, parallel uniformly distributed
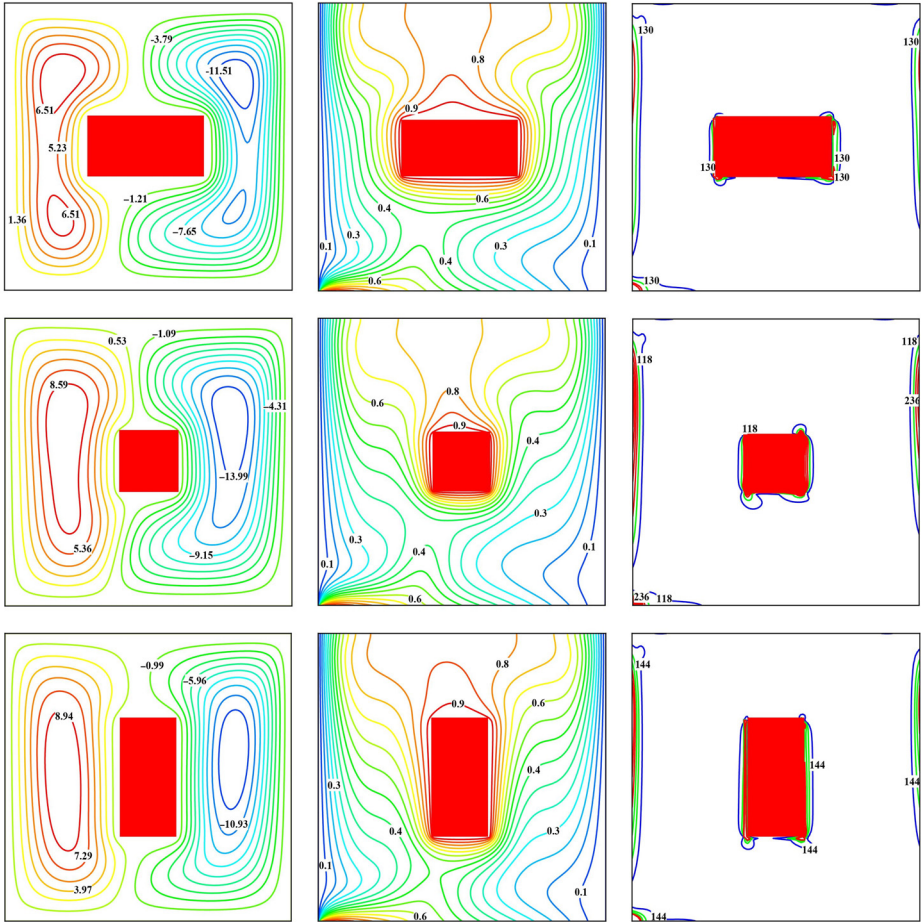
Figure 5.
Streamlines (left),
isotherms (middle)
and S_{GEN} (right) for
$\Gamma = 0.5$ (row-I), $\Gamma = 1.0$ (row-II), $\Gamma = 2.0$ (row-III) at $Ra = 10^5$,
$\phi = 0.04$ with linear
heating

Source: Figure by authors

thermal contours are formed in the vertical sides of the block due to the passage between block and side walls. Also, the isothermal structure indicates that block aspect ratio has no remarkable impact on the thermal field. As regards to irreversibility distribution, the variation in hot block aspect ratio has minimal impact on the entropy contour pattern; however, the change in magnitude of EG has been noticed. It has been found that the minimal EG is achieved with square hot block compared to shallow and tall blocks.

4.2 Cup-mixing temperature

The influence of various parameters on the cup-mixing temperature which describes the thermal distribution uniformity denoted by T_{cup} has been illustrated in Figures 6 and 7. The impact of Rayleigh number for different solid block size, aspect ratio of the block and nanoparticle shape subjected to three thermal boundary conditions is illustrated in Figure 6.

It reveals that lower T_{cup} is found at $Ra = 10^3$ due to lower thermal distribution with respect to weaker streamlines. As Ra is enhanced, flow velocity increases and produces stronger flow circulation and in turn enhancing the cup-mixing temperature in the enclosure. It has been found that during stronger convection, maximum cup-mixing temperature is noticed to be at moderate obstacle size ($h = d = 0.5$) irrespective of thermal profile, and it is interesting to note that at this particular choice, the spherical shaped nanoparticles provide maximum thermal uniformity compared to other chosen shapes (displayed in Figure 7). In regard to hot block aspect ratio, the variation in cup-mixing temperature reveals a nonuniform structure. This prediction suggests that the values for h and d of the block should be preferred than other parameters. It also noticed that irrespective of controlling parameters, uniform bottom wall heating produces higher magnitude of T_{cup}, indicating an enhanced thermal uniformity in the annulus followed by sinusoidal and linear conditions.

4.3 Average Nusselt number
Figures 8 and 9 illustrate the variation of overall Nu for vast range of parametric values. Irrespective of nanoparticle shape and other parametric values, the HTR has been increased with an increment in Ra. It is attributed to enhanced buoyant force generated from larger
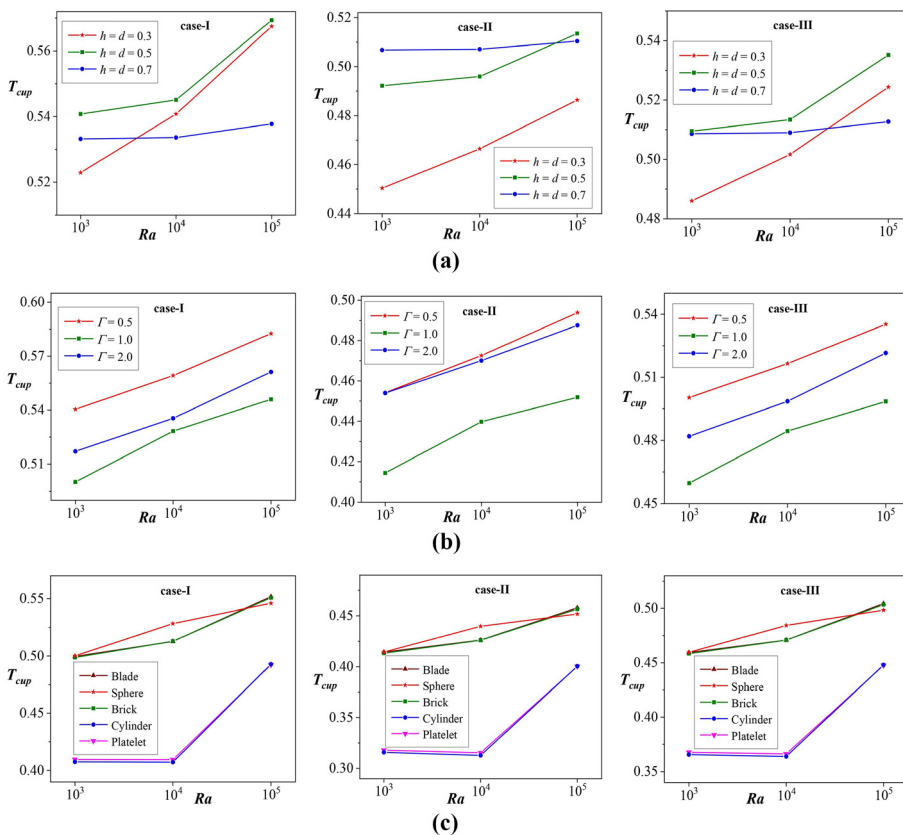
Figure 6.
Effect of Ra and (a) h at $\Gamma = 1$, $\phi = 0,05$, (b) Γ at $\phi = 0.05$ and (c) nanoparticle shape at $d = h = 0.2$, $\phi = 0.05$, $\Gamma = 1$ on cup-mixing temperature for different thermal boundary conditions
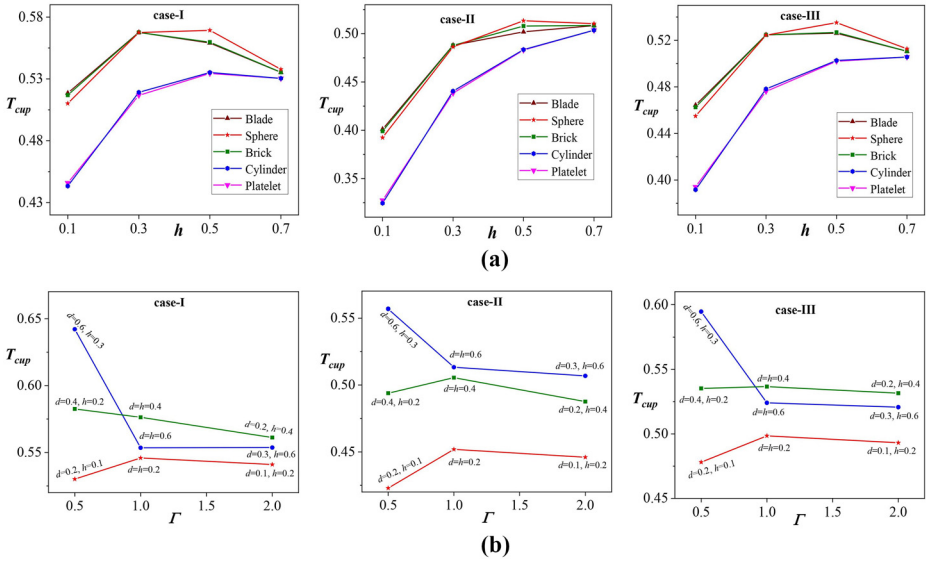
Source: Figure by authors

Source: Figure by authors

thermal gradients produced in the annulus. Among three different block sizes considered in this analysis, the maximum thermal dissipation has been predicted with a smaller block. Physically, this could be interpreted due to maximum fluidity in the space between block and annular boundaries. In addition, it has also been noticed that the variation in HTR with Rayleigh number is meager for the largest block considered in the analysis. This is because, the maximum annular region has been occupied by the hot block which restricts the nanofluid movement and hence leads to convection–conduction transition mode. For the same block size, similar phenomenon has been noticed in all three thermal boundary conditions. Also, the study has been carried out for $\Gamma = 0.5$ ($d = 0.4$, $h = 0.2$), $\Gamma = 1.0$ ($d = h = 0.2$) and $\Gamma = 2.0$ ($d = 0.2$, $h = 0.4$). It has been noticed that during convection dominant mode ($Ra > 10^4$), among three different Γ values, regardless of thermal boundary condition, maximum energy transport is observed with unit Γ and minimum heat dissipation with $\Gamma = 0.5$. This might be due to shorter distance between cold surface of vertical wall and hot surface of solid block. Furthermore, the influence of nanoparticle shape on average Nu has been studied by fixing all other parameters. It is interesting to note that the spherical shaped nanoparticle gives higher thermal transfer rate with uniform heating, whereas the blade-shaped nanoparticles perform well with nonuniform thermal boundary condition (linear and sinusoidal). This reveals that the shape of nanoparticle should be carefully chosen depending upon the thermal conditions. In addition to this, it also reveals that the cylinder- and platelet-shaped nanoparticles give poor performance in heat dissipation rate due to higher viscosity. This study has been extended for different block sizes, and variation in $\overline{Nu}$ has been displayed in Figure 9 for fixed $Ra = 10^5$, $\Gamma = 1$. It is very interesting to note that the HTR decreases against block size with sphere-shaped nanoparticles, while for the other nanoparticle shapes, the thermal dissipation rate enhances with the block size. In Case-II and Case-III, the blade shape exhibits greater $\overline{Nu}$, while in Case-I, the sphere-shaped nanoparticle augments the global Nu for $h \leq 0.5$. The above predictions suggest that much focus should be given in choosing the nanoparticle shape to increase the thermal
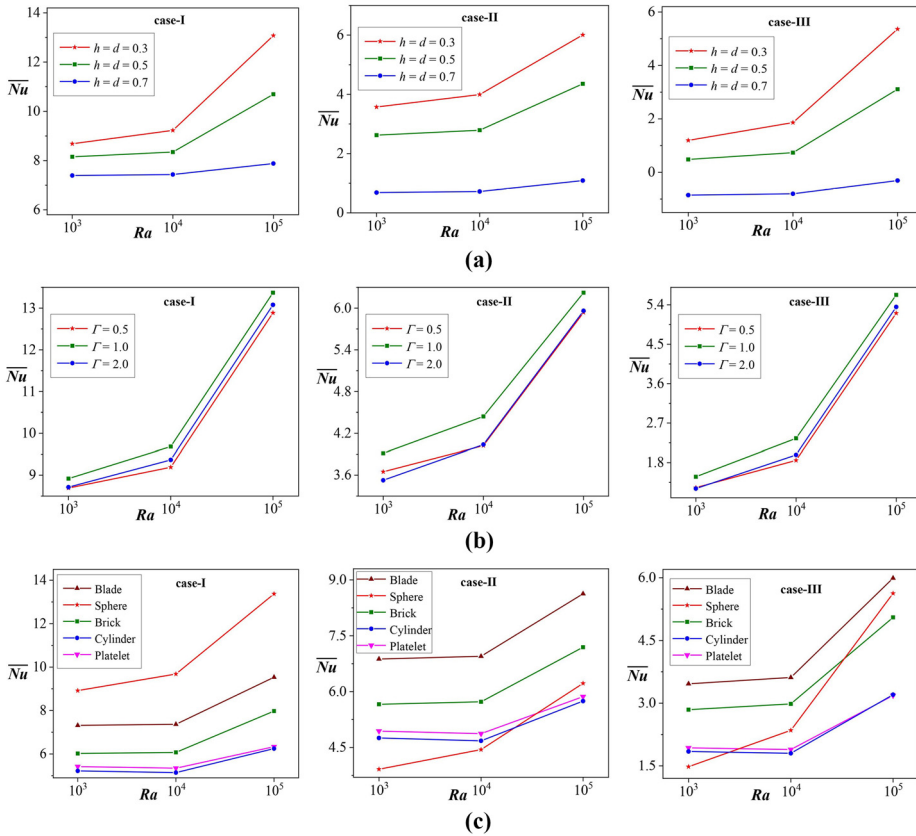
Source: Figure by authors

transport performance. Finally, the impact of hot block size (various lengths and heights) and aspect ratio on $\overline{Nu}$ has been studied and found that unit Γ value exhibits lower thermal transport performance compared to other Γ values. However, in Figure 9(b) increase in Γ from 0.5 to 2.0 has been made by enhancing the block height, while in Figure 8(b), it has been made by decreasing the block width. Therefore, it can be concluded that choosing the size of hot solid block plays key role in increasing the HTR. In general, through Figures 8 and 9, it has been detected that the bottom wall with uniform heating dissipates maximum thermal energy compared to other boundary conditions.

4.4 Total entropy generation

In all energy transport phenomena, which occur due to thermal difference, the EG could not be avoided. However, this quantity should be minimized to enhance the system efficiency. In this regard, a computational investigation has been performed for examining the optimum value of parameters to minimize S_{tot} and is portrayed in Figures 10 and 11. The effect of Rayleigh number on S_{tot} for different parameters has been illustrated in Figure 10 with 5% of nanoparticle volume fraction. It has been noticed that enhancement of Ra from 10^3 to 10^4 does
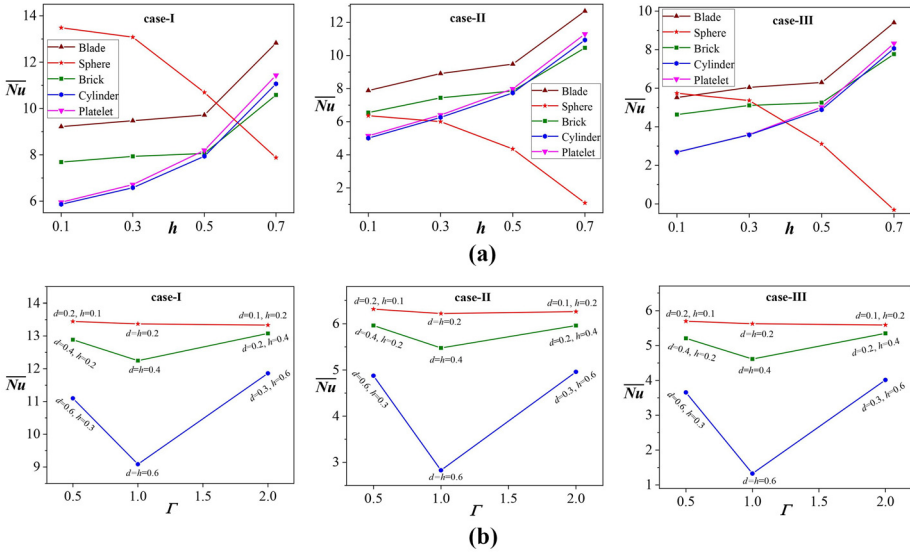
Source: Figure by authors

not show a significant change in EG; however, on enhancement of Ra to 10^5, a profound increase in S_{tot} has been identified. This is because, at lower and moderate Ra, conduction dominates convection and hence the fluidity and friction entropy is expected to be less, but with $Ra = 10^5$, fluidity has been found to be greater and hence S_{tot} enhances. It is interesting to note that during conduction dominant mode ($Ra \leq 10^4$), with respect to obstacle size, minimum and maximum EG is detected for smaller and larger block sizes, respectively, while the reverse is observed at convective mode. The obstacle aspect ratio influence on S_{tot} has been illustrated in Figure 10(b). The study has been addressed by taking three different aspect ratios ($\Gamma = 0.5$, $\Gamma = 1.0$ and $\Gamma = 2.0$) into consideration. It reveals that the aspect ratio of the block does not show significant change in S_{tot}. For the choice of parameters considered in Figure 10(b), minimal S_{tot} has been found to be with $\Gamma = 0.5$. In regard to nanoparticle shape, it has been found that at lower and moderate Rayleigh number ($Ra = 10^3$ and 10^4), nanoparticle shape does not show significant variation in total EG, whereas enhancement in EG results with an increase in Ra. This is due to the fact that shape factor of the nanoparticle shows significant effect on flow strength that occurs during convective mode. Among the five different nanoparticle shapes considered, maximum EG is noticed with spherical shaped nanoparticles. The same mechanism is observed for uniform and nonuniform thermal conditions. This investigation has been made by considering different sizes of hot block with $\Gamma = 1$, and variation in S_{tot} has been displayed in Figure 11(a). It has been noticed that the sphere-, blade- and brick-shaped nanoparticles produce a decrease in S_{tot} with an increase in block size during uniform bottom wall heating, while, with nonuniform thermal profile, EG enhances, reaches maximum and declines with an increase in hot block size. This decrease in total EG is due to decrease in friction entropy caused due to larger solid block. However, enhancement of hot block size from 0.1 to 0.7 enhances the total EG for cylinder as well as platelet shaped nanoparticles. The physical interpretation for this observation could be that the viscosity of nanoliquid for cylinder- and platelet-shaped nanoparticles is greater due to which the fluidity will be minimum; moreover, an enhancement of block size leads to an increase in HTE, and this
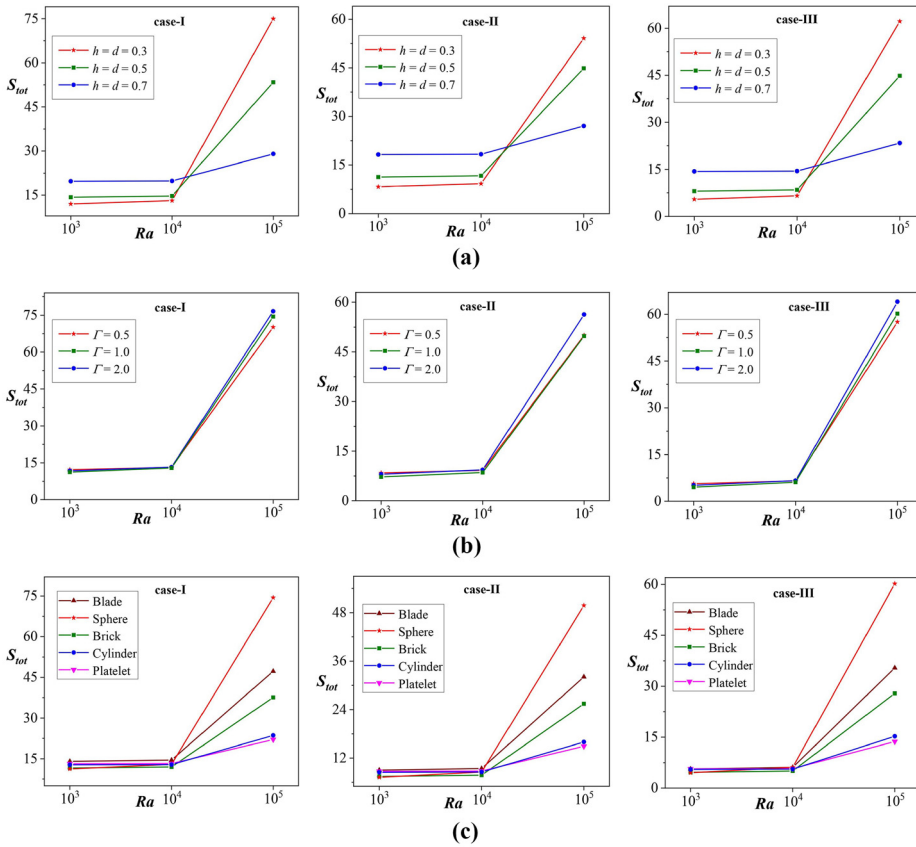
Source: Figure by authors

results in enhancement of total EG and is true for all thermal profiles. The effect of different block size for each Γ on S_{tot} has been displayed in Figure 11(b) by fixing $Ra = 10^5$ and $\phi = 0.05$. It has been observed that minimum EG has been achieved with different aspect ratios for each size of the block. This concludes that along with the aspect ratio of the hot solid block, the size also is a significant factor in suppressing total EG in the enclosure.

4.5 Average Bejan number

The Bejan number is a dimensionless quantity that predicts the contribution of individual components to total EG in the enclosure, also Be is the ratio of heat transfer entropy to sum of heat transfer and friction entropy. If the value of Be is greater than 0.5, it is worth to mention that HTE is contributing maximum to the total EG and for $Be < 0.5$, FFE is contributing more to total EG. The wide range of parametric study has been performed and is displayed in Figures 12 and 13 to analyze the individual component contribution to total EG. The effect of Ra on Be for different parameters has been illustrated in Figure 12, with 5% of nanoparticle volume fraction. Irrespective of parametric values and nanoparticle
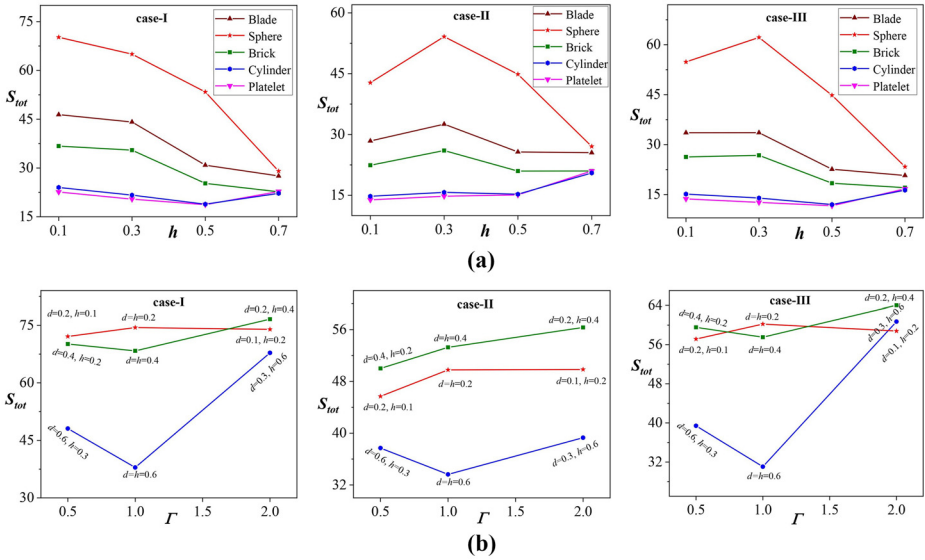
Figure 11.
Effect of (a)
nanoparticle shape
and hot block size at
$Ra = 10^5, \Gamma = 1, \phi =$
0.05 and (b) Γ and hot
block size at $Ra =$
$10^5, \phi = 0.05$, on total
entropy generation
for different thermal
boundary conditions

Source: Figure by authors

shape, Be is found to be greater than or equal to 0.5 ($Be \geq 0.5$) at $Ra \leq 10^4$, while at $Ra = 10^5$, Be is found to be less than 0.5. This indicates that, during conduction-dominant mode, HTE is dominant and during convection mode, FFE is contributing more than HTE. The physical reason behind this mechanism is Be is inversely proportional to S_{tot} [refer equation (11)]. Because of this reason, the average Bejan number in the study of nanoparticle shape effect, obstacle size and aspect ratio of hot block is noticed to be less than 0.5 (Figure 13), but in some cases, Be values lies between 0.45 and 0.6. In such situations, we can conclude that the HTE and FFE are nearly equal.

4.6 Performance evaluation criteria
The key objective of this computation is to examine the optimum values of parameters at which greater energy dissipation takes place with minimum EG, which is essential in any thermal device. This could be predicted by estimating the parameter known as PEC which is the ratio of HTR to EG. In the present investigation, the major critical parameters are size of the hot block, nanoparticle shape and thermal boundary condition whose impacts on PEC are examined in Figure 14 for various reference samples. In general, greater the PEC value, greater the system thermal performance. Figure 14 shows the PEC for different nanoparticle shape for various hot block size and bottom wall thermal boundary condition. The evaluated PEC value reveals that the enrichment of hot block size leads to an enhancement in PEC, except for spherical nanoparticle shape. Among the various combinations of thermal boundary condition, nanoparticle shape and hot block size, it has been found that the nanoliquid prepared using platelet shaped nanoparticle gives better PEC value. However, the viscosity of these fluids is found to be high due to which the fluidity and associated HTR will be minimal. Therefore, among blade-, sphere- and brick-shaped nanoparticles, PEC value is found to be greater for blade shape. Hence, usage of blade-shaped nanoparticles to
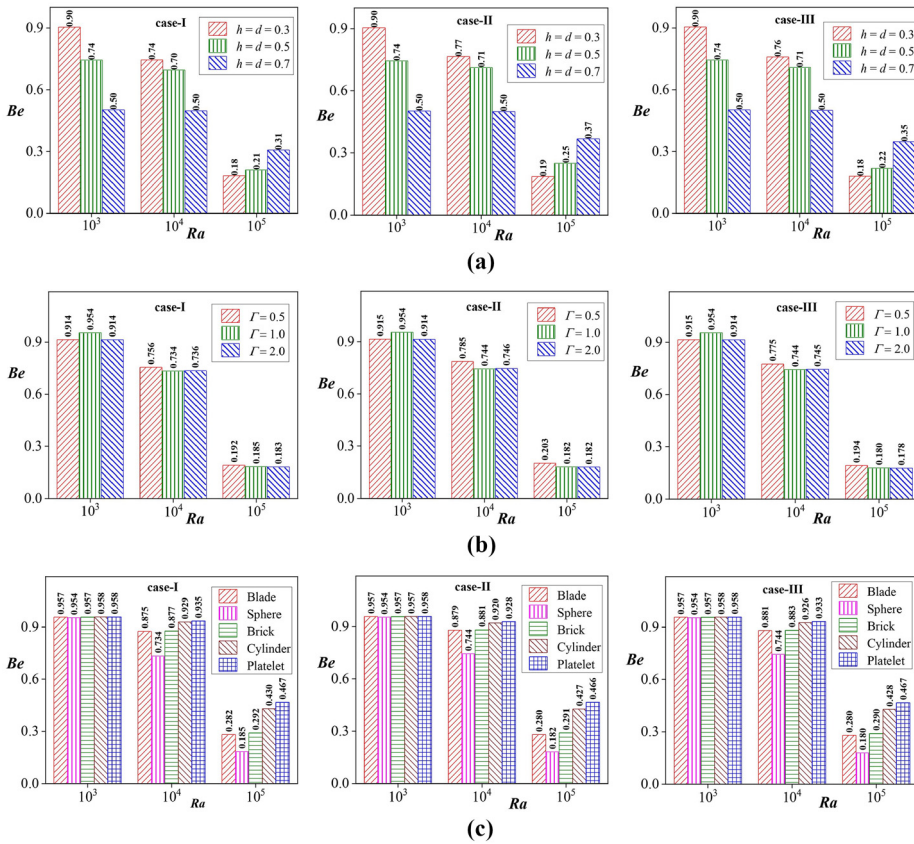
Source: Figure by authors

prepare nanoliquid gives better thermal performance with greater system efficiency (maximum heat dissipation rate with minimum EG).

5. Conclusions
Buoyant convective heat transfer and irreversibility distribution of $Ag - H_2O$ nanoliquid filled in a cylindrical annulus with a hot obstacle mounted at the center of the geometry has been numerically analyzed. The impact of effective parameters such as Rayleigh number, nanoparticle shape, size and aspect ratio of hot block on liquid flow, thermal lines, heat dissipation rate, S_{tot} and Be has been investigated for different source–sink locations and presented via graphs. The interesting findings of this investigation are as follows:

- The variation in Rayleigh number leads to change in the mode of heat transfer and hence profound variation in the liquid movement pattern, thermal and entropy distribution fields has been detected in the annulus. It has been noticed that regardless to size of the hot block, nanoparticle shape and bottom wall thermal condition, enhancement of Rayleigh number increases the heat dissipation rate, cup-mixing temperature and total EG in the enclosure.
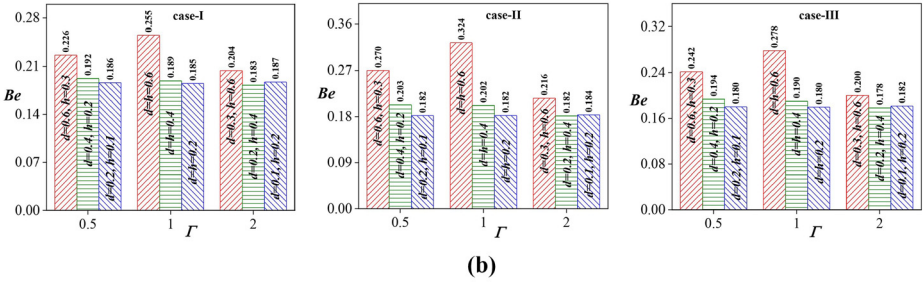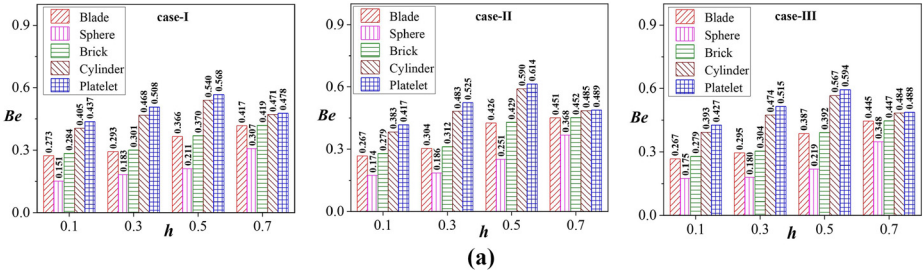
Figure 13.
Effect of (a)
nanoparticle shape
and hot block size at
$Ra = 10^5$, $\Gamma = 1$, $\phi =$
0.05, (b) Γ and hot
block size at $Ra =$
10^5, $\phi = 0.05$, on
Bejan number for
different thermal
boundary conditions
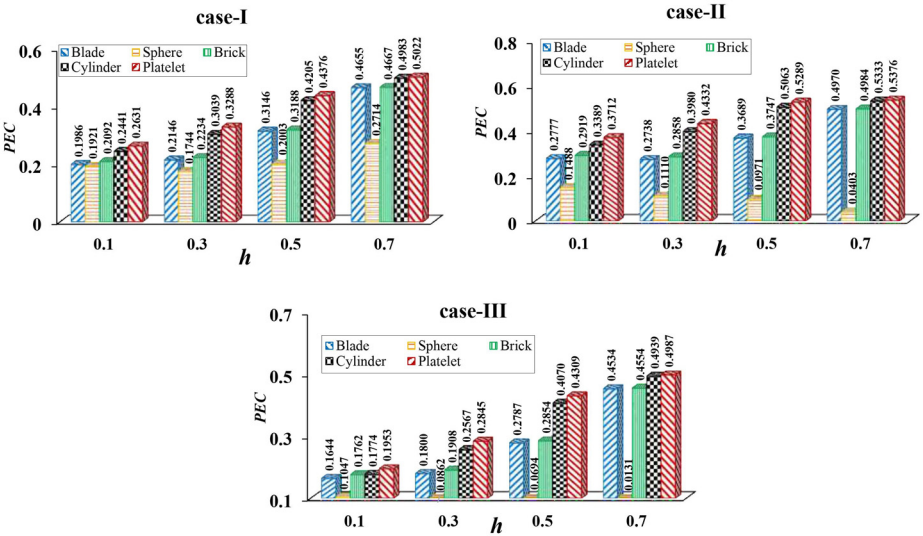
Source: Figure by authors

Figure 14.
Effect of hot block
size and nanoparticle
shape on
performance
evaluation criteria
(PEC) at $Ra = 10^5$,
$\phi = 0.05$, $\Gamma = 1$ for
different thermal
boundary conditions

Source: Figure by authors

- The nanoparticle shape which varies the viscosity of nanoliquid has major impact on heat dissipation rate. It is quite interesting to note that the spherical shaped nanoparticles decline HTR and EG with increase on hot block size, while an increment in HTR and decrease in EG has been noticed with other nanoparticle

shapes. However, the cup-mixing temperature for all nanoparticle shapes enhances up to a certain point and then decreases.

- On varying the aspect ratio of block, the distance between hot block and cooled vertical surfaces decreases and hence change in thermal gradients is observed, resulting in variation in flow strength and heat dissipation rate. The impact of block aspect ratio is quite complicate because, the maximum flow strength, heat dissipation and cup-mixing temperature are not obtained with same aspect ratio. However, maximum entropy is generated with tall hot obstacle irrespective of bottom wall boundary condition.
- The another major parameter in this analysis is the size of hot block mounted at the annulus center. A profound change in nanoliquid flow, thermal distribution and EG pattern has been noticed with enhancement of hot block size. As the size of the block has been increased, conduction-dominant takes place due to which the flow strength declines and results in 53.43% and 57.92% decrease of HTR and total EG, respectively.
- The prime objective of the present analysis is to identify the set of parameters to maximize the heat transport and minimize EG. From the vast numerical simulations, we have observed that the PEC is greater for annulus with larger obstacle, and this holds good for all considered thermal boundary conditions.

References

Abouali, O. and Falahatpisheh, A. (2009), "Numerical investigation of natural convection of Al$_2$O$_3$ nanofluid in vertical annuli", *Heat and Mass Transfer*, Vol. 46 No. 1, pp. 15-23.

Alsabery, A.I., Ishak, M.S., Chamkha, A.J. and Hashim, I. (2018), "Entropy generation analysis and natural convection in a nanofluid-filled square cavity with a concentric solid insert and different temperature distributions", *Entropy*, Vol. 20 No. 5, p. 336.

Baytas, A.C. (2000), "Entropy generation for natural convection in an inclined porous cavity", *International Journal of Heat and Mass Transfer*, Vol. 43 No. 12, pp. 2089-2099.

Bejan, A. (1982), "Second-law analysis in heat and thermal design", *Advances in Heat Transfer*, Vol. 15, pp. 1-58.

Bejan, A. (1996), *Entropy Generation Minimization*, CRC Press, Boca Raton, FL.

Belhaj, S. and Ben-Beya, B. (2022), "Thermal performance analysis of hybrid nanofluid natural convection in a square cavity containing an elliptical obstacle under variable magnetic field", *International Journal of Numerical Methods for Heat and Fluid Flow*, Vol. 32 No. 6, pp. 1825-1860.

Berrahil, F., Filali, A., Abid, C., Benissaad, S., Bessaih, R. and Matar, O. (2021), "Numerical investigation on natural convection of Al$_2$O$_3$/water nanofluid with variable properties in an annular enclosure under magnetic field", *International Communications in Heat and Mass Transfer*, Vol. 126, p. 105408.

Choi, S.U.S. and Eastman, J.A. (1995), "Enhancing thermal conductivity of fluids with nanoparticles", ASME International Mechanical Engineering Congress and Exhibition.

Dogonchi, A.S. and Hashim, (2019), "Heat transfer by natural convection of Fe$_3$O$_4$-water nanofluid in an annulus between a wavy circular cylinder and a rhombus", *International Journal of Heat and Mass Transfer*, Vol. 130, pp. 320-332, doi: 10.1016/j.ijheatmasstransfer.2018.10.086.

Dogonchi, A.S., Mishra, S.R., Chamkha, A.J., Ghodrat, M., Elmasry, Y. and Alhumade, H. (2021), "Thermal and entropy analyses on buoyancy-driven flow of nanofluid inside a porous enclosure with two square cylinders: finite element method", *Case Studies in Thermal Engineering*, Vol. 27, p. 101298.

Esfe, M.H., Arani, A.A.A., Karimipour, A. and Esforjani, S.S.M. (2014), "Numerical simulation of natural convection around an obstacle placed in an enclosure filled with different types of nanofluids", *Heat Transfer Research*, Vol. 45 No. 3, pp. 279-292.

Godson, L., Raja, B., Lal, D.M. and Wongwises, S. (2010), "Enhancement of heat transfer using nanofluids – an overview", *Renewable and Sustainable Energy Reviews*, Vol. 14 No. 2, pp. 629-641.

Hamad, F.A.W. (1989), "Experimental study of natural convection heat transfer in inclined cylindrical annulus", *Solar and Wing Technology*, Vol. 6 No. 6, pp. 573-579.

Hamzah, H. and Sahin, B. (2023), "Analysis of SWCNT-water nanofluid flow in wavy channel under turbulent pulsating conditions: investigation of homogeneous and discrete phase models", *International Journal of Thermal Sciences*, Vol. 184, p. 108011.

House, J.M., Beckermann, C. and Smith, T.F. (1990), "Effect of a centered conducting body on natural convection heat transfer in an enclosure", *Numerical Heat Transfer, Part A: Applications*, Vol. 18 No. 2, pp. 213-225.

Ilis, G.G., Mobedi, M. and Sunden, B. (2008), "Effect of aspect ratio on entropy generation in a rectangular cavity with differentially heated vertical walls", *International Communications in Heat and Mass Transfer*, Vol. 35 No. 6, pp. 696-703.

Kardgar, A. (2021), "Numerical investigation of conjugate heat transfer and entropy generation of MHD natural convection of nanofluid in an inclined enclosure", *International Journal of Numerical Methods for Heat and Fluid Flow*, Vol. 31 No. 1, pp. 308-344.

Kim, B.S., Lee, D.S., Ha, M.Y. and Yoon, H.S. (2008), "A numerical study of natural convection in a square enclosure with a circular cylinder at different vertical locations", *International Journal of Heat and Mass Transfer*, Vol. 51 No. 7-8, pp. 1888-1906.

Kumar, A.V., Lawrence, J. and Saravanakumar, G. (2022a), "Fluid friction/heat transfer irreversibility and heat function study on MHD free convection within the MWCNT-water nanofluid-filled porous cavity", *Heat Transfer*, Vol. 51 No. 5, pp. 4247-4267.

Kumar, V., Murthy, S. and Kumar, B.V.R. (2022b), "Entropy generation in a chemically and thermally reinforced doubly stratified porous enclosure in a magnetic field", *Physics of Fluids*, Vol. 34 No. 1, p. 13307.

Kumar, A., Dash, A.P., Ray, A.K., Sethy, P. and Kasireddy, I. (2023), "Unsteady mixed convective flow of hybrid nanofluid past a rotating sphere with heat generation/absorption: an impact of shape factor", *International Journal of Numerical Methods for Heat and Fluid Flow*, doi: 10.1108/HFF-03-2023-0129.

Lakshmi, K.M., Laroze, D. and Siddheshwar, P.G. (2021), "A study of the natural convection of water-AA7075 nanoliquids in low-porosity cylindrical annuli using a local thermal non-equilibrium model", *Physics of Fluids*, Vol. 33 No. 3, p. 32018.

Lopez, J.M. and Marques, F. (2014), "Three-dimensional instabilities in a discretely heated annular flow: onset of spatio-temporal complexity via defect dynamics", *Physics of Fluids*, Vol. 26 No. 6, p. 64102.

Mahmoodi, M. and Sebdani, S.M. (2012), "Natural convection in a square cavity containing a nanofluid and an adiabatic square block at the center", *Superlattices and Microstructures*, Vol. 52 No. 2, pp. 261-275.

Malik, S. and Nayak, A.K. (2017), "MHD convection and entropy generation of nanofluid in a porous enclosure with sinusoidal heating", *International Journal of Heat and Mass Transfer*, Vol. 111, pp. 329-345.

Manna, N.K., Mondal, C., Biswas, N., Sarkar, U.K., Oztop, H.F. and Abu-Hamdeh, N.H. (2021), "Effect of multibanded magnetic field on convective heat transport in linearly heated porous systems filled with hybrid nanofluid", *Physics of Fluids*, Vol. 33 No. 5, p. 53604.

Mebarek-Oudina, F. (2019), "Convective heat transfer of titania nanofluids of different base fluids in cylindrical annulus with discrete heat source", *Heat Transfer—Asian Research*, Vol. 48 No. 1, pp. 135-147.

Mirzaie, M. and Lakzian, E. (2021), "Natural convection of nanofluid-filled annulus with cooled and heated sources and rotating cylinder in the water near the density inversion point", *European Physical Journal plus*, Vol. 136, p. 834.

Mun, G.S., Doo, J.H. and Ha, M.Y. (2016), "Thermo-dynamic irreversibility induced by natural convection in square enclosure with inner cylinder. Part-I: effect of tilted angle of enclosure", *International Journal of Heat and Mass Transfer*, Vol. 97, pp. 1102-1119.

Pal, G.C., Nammi, G., Pati, S., Randive, P.R. and Baranyi, L. (2022), "Natural convection in an enclosure with a pair of cylinders under magnetic field", *Case Studies in Thermal Engineering*, Vol. 30, p. 101763.

Prasad, V. and Kulacki, F.A. (1985), "Free convection heat transfer in a liquid-filled annulus", *Journal of Heat Transfer*, Vol. 107 No. 3, pp. 596-602.

Ragui, K., Benkahla, Y., Labsi, N. and Boutra, A. (2013), "Natural heat transfer convection in a square cavity including a square heater", *Proceedings of the 21st French Congress of Mechanics*, Bordeaux, France.

Rahmati, A.R. and Tahery, A.A. (2018), "Numerical study of nanofluid natural convection in a square cavity with a hot obstacle using lattice Boltzmann method", *Alexandria Engineering Journal*, Vol. 57 No. 3, pp. 1271-1286.

Reddy, N.K. and Sankar, M. (2023), "Buoyant heat transfer of nanofluids in a vertical porous annulus: a comparative study of different models", *International Journal of Numerical Methods for Heat and Fluid Flow*, Vol. 33 No. 2, pp. 477-509.

Reddy, N.K., Swamy, H.A.K. and Sankar, M. (2021), "Buoyant convective flow of different hybrid nanoliquids in a non-uniformly heated annulus", *The European Physical Journal Special Topics*, Vol. 230 No. 5, pp. 1213-1255.

Rosca, A.V., Rosca, N.C., Pop, I. and Sheremet, M.A. (2023), "Natural convection and entropy generation in a trapezoidal region with hybrid nanoliquid under magnetic field", *International Journal of Numerical Methods for Heat and Fluid Flow*, doi: 10.1108/HFF-04-2023-0193.

Roy, N.C. (2019), "Flow and heat transfer characteristics of a nanofluid between a square enclosure and a wavy wall obstacle", *Physics of Fluids*, Vol. 31 No. 8, p. 82005.

Saha, L.K., Bala, S.K. and Roy, N.C. (2020), "Natural convection of dusty nanofluids within a concentric annulus", *European Physical Journal Plus*, Vol. 135, p. 732.

Sankar, M. and Do, Y. (2010), "Numerical simulation of free convection heat transfer in a vertical annular cavity with discrete heating", *International Communications in Heat and Mass Transfer*, Vol. 37 No. 6, pp. 600-606.

Sankar, M., Swamy, H.A.K., Al-Mdallal, Q. and Wakif, A. (2023), "Non-Darcy nanoliquid buoyant flow and entropy generation analysis in an inclined porous annulus: effect of source-sink arrangement", *Alexandria Engineering Journal*, Vol. 68, pp. 239-261.

Selimefendigil, F. and Oztop, H.F. (2015), "Natural convection and entropy generation of nanofluid filled cavity having different shaped obstacles under the influence of magnetic field and internal heat generation", *Journal of the Taiwan Institute of Chemical Engineers*, Vol. 56, pp. 42-56.

Sheikhzadeh, G.A., Nikfar, M. and Fattahi, A. (2012), "Numerical study of natural convection and entropy generation of Cu-water nanofluid around an obstacle in a cavity", *Journal of Mechanical Science and Technology*, Vol. 26 No. 10, pp. 3347-3356.

Sheremet, M., Pop, I., Oztop, H.F. and Abu-Hamdeh, N. (2017), "Natural convection of nanofluid inside a wavy cavity with a non-uniform heating entropy generation analysis", *International Journal of Numerical Methods for Heat and Fluid Flow*, Vol. 27 No. 4, pp. 958-980.

Shuja, S.Z., Yilbas, B.S. and Budair, M.O. (2000), "Natural convection in a square cavity with heat generating body: entropy consideration", *Heat and Mass Transfer*, Vol. 36 No. 4, pp. 343-350.

Tayebi, T. and Chamkha, A.J. (2020), "Entropy generation analysis during MHD natural convection flow of hybrid nanofluid in a square cavity containing a corrugated conducting block", *International Journal of Numerical Methods for Heat and Fluid Flow*, Vol. 30 No. 3, pp. 1115-1136.

Tayebi, T., Dogonchi, A.S., Chamkha, A.J., Hamida, M.B.B., El-Sapa, S. and Galal, A.M. (2022), "Micropolar nanofluid thermal free convection and entropy generation through an inclined I-shaped enclosure with two hot cylinders", *Case Studies in Thermal Engineering*, Vol. 31, p. 101813.

Vijaybabu, T.R. (2020), "Influence of permeable circular body and Cu−H$_2$O nanofluid on buoyancy-driven flow and entropy generation", *International Journal of Mechanical Sciences*, Vol. 166, p. 105240.

Yan, S., Pordanjani, A.H., Aghakhani, S., Goldanlou, A.S. and Afrand, M. (2020), "Effect of nano powder shapes on natural convection of nanofluids inside a square enclosure in presence of fins with different shapes and magnetic field effect", *Advanced Powder Technology*, Vol. 31 No. 7, pp. 2759-2777.

Corresponding author
Younghae Do can be contacted at: yhdo@knu.ac.kr